Coherent anti-Stokes Raman scattering (CARS) microscopy of fluid inclusions: multimodal 3D, chemically selective imaging and spectroscopy

Burruss, Robert C.*, Slepkov, Aaron D.**, Pegoraro, Adrian F.** and Stolow, Albert**

*US Geological Survey, Reston, VA 20191 USA
**National Research Council of Canada, Ottawa, Ontario, Canada

3D images and spectra of hydrocarbon and aqueous fluid inclusions have been recorded for the first time with coherent anti-Stokes Raman scattering (CARS) and associated nonlinear optical microscopy methods, second harmonic generation (SHG) and two-photon excitation fluorescence (TPEF). Laser scanning confocal microscopy (LSCM) with CARS is primarily used for biomedical imaging of lipids using the C-H stretching vibration (Pegararo, et al., 2010) suggesting that it should be able to image CH_4 in fluid inclusions. The CARS microscope uses a single ultrafast laser source that simultaneously generates SHG and TPEF images with the CARS image (Pegoraro, et al., 2010). All three signals are generated in the same focal volume and are collected on separate detectors, creating high-resolution 3-D images that complement the chemically-specific CARS image. The TPEF signal images the distribution of aromatic hydrocarbons and the SHG signal is sensitive to crystallographic disorder and internal surfaces in host minerals providing 3D images of inclusion shape, microfractures and grain boundaries. In the current configuration of the CARS system, images and spectra can be recorded from 2100 to 4500 cm^{-1}, providing observations for N_2, H_2S, CH_4, H_2O, and H_2. The coherent properties of the CARS signal provide orders of magnitude more signal than conventional spontaneous Raman scattering, allowing images to be acquired at about 5 microseconds/voxel. Image volumes of 350 x 350 x 100 micrometers can be recorded in minutes and hyperspectral image volumes can be recorded in less than 10 minutes.

We tested the system with CH_4-rich, CH_4-H_20, and petroleum inclusions in sedimentary, igneous, and metamorphic rocks. 3D images of CH_4 and water clearly identify aqueous inclusions with CH_4-rich vapour bubbles that coexist with one-phase CH_4-rich inclusions (Fig. 1). In crude oil inclusions, CARS spectra of CH_4 (Fig. 2) are clearly separated from fluorescence emission of the oil.

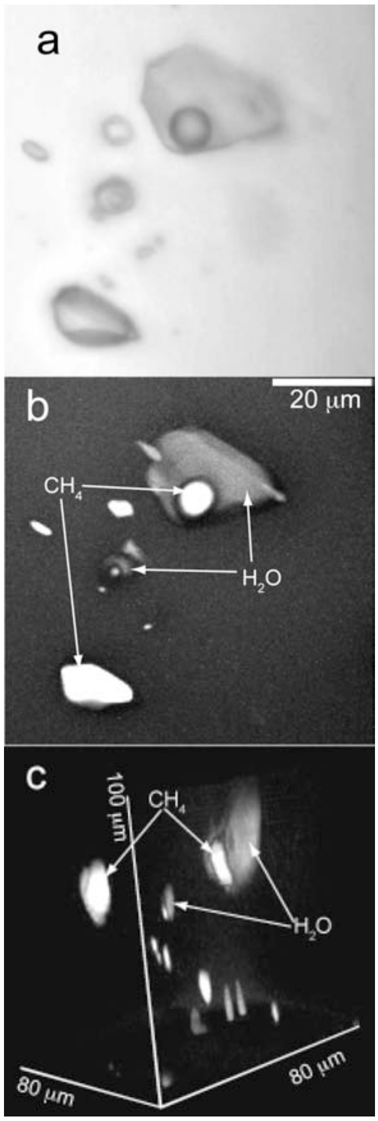

Fig. 1. CH_4-rich and CH_4- H_2O inclusions imaged in CARS. (a) Transmitted light, flattened Z-stack of multiple focal planes. (b) Flattened Z-stack, CARS image, white, CH_4 at 2910 cm^{-1}; medium grey, H_2O at 3450 cm^{-1}. (c) 3D projection of (b) rotated clockwise approximately 90^o.

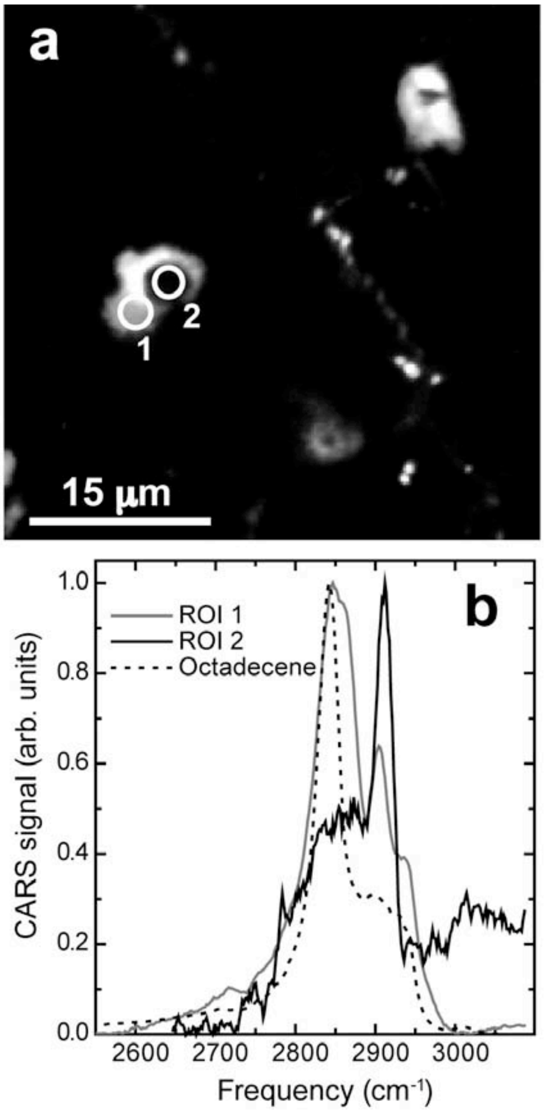

Fig. 2. Combined CARS (~2830 cm^{-1}) and TPEF (grey to white) image of 2-phase oil inclusions in calcite (a) with regions of interest (ROI) where CARS spectra (b) were recorded. Spectrum of the liquid phase (ROI 1, grey curve) has a peak for CH_4 in solution in the oil, whereas the spectrum of the vapour phase (ROI 2, black curve) has a more intense peak for CH_4 at slightly higher wavenumber. The dashed curve is a reference spectrum of octadecene.

This allows the pressure sensitive peak position of CH_4 (Lu, *et al.*, 2007) in oil inclusions to be recorded for the first time, providing crucial input to PVT models of oil migration. Surprisingly, some CH_4-rich inclusions in metamorphic and igneous rocks show TPEF signals that indicate the presence of aromatic hydrocarbons associated with CH_4 in these environments. Healed microfractures are visible in SHG (Fig. 3) allowing identification of distinct generations of CH_4-rich inclusions associated with specific fracture orientations.

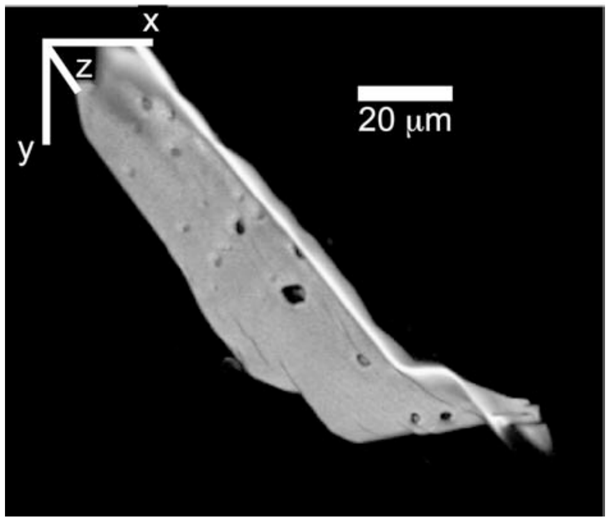

Fig. 3. 3D projection of SHG image of healed microfracture in quartz (grey) decorated with CH_4-rich fluid inclusions (dark grey, CARS).

We believe these initial results demonstrate the broad potential of multimodal CARS microscopy to take fluid inclusion studies to new dimensions of chemical and spatial detail. In addition to analysis of fluid inclusions, these imaging methods are applicable to a wide range of geoscience applications in biogeochemistry, geobiology, mineralogy, and diagenesis.

REFERENCES

Pegoraro *et al.* (2010) *App. Phys.* 49, F10-F17.

Lu, *et al.* (2007) *Geochim. Cosmo. Acta* 71, 3969 - 3978.